PHOTONICS Research

Surface ligand modified cesium lead bromide/silica sphere composites for low-threshold upconversion lasing

QIAN XIONG,[1,2,3,4] SIHAO HUANG,[1] ZIJUN ZHAN,[2] JUAN DU,[1,2,5,7] XIAOSHENG TANG,[6,8] ZHIPING HU,[2] ZHENGZHENG LIU,[1] ZEYU ZHANG,[2] WEIWEI CHEN,[6] AND YUXIN LENG[1,2,3,9]

[1]State Key Laboratory of High Field Laser Physics and CAS Center for Excellence in Ultra-intense Laser Science, Shanghai Institute of Optics and Fine Mechanics (SIOM), Chinese Academy of Sciences (CAS), Shanghai 201800, China
[2]Hangzhou Institute for Advanced Study, University of Chinese Academy of Sciences, Hangzhou 310024, China
[3]School of Physical Science and Technology, ShanghaiTech University, Shanghai 201210, China
[4]Center of Materials Science and Optoelectronics Engineering, University of Chinese Academy of Sciences, Beijing 100049, China
[5]School of Physics and Electronics, Shandong Normal University, Jinan 250014, China
[6]College of Optoelectronic Engineering, Chongqing University of Post and Telecommunications, Chongqing 400065, China
[7]e-mail: dujuan@mail.siom.ac.cn
[8]e-mail: xstang@cqupt.edu.cn
[9]e-mail: lengyuxin@mail.siom.ac.cn

Received 14 September 2021; revised 16 November 2021; accepted 29 December 2021; posted 4 January 2022 (Doc. ID 442659); published 9 February 2022

In recent years, all-inorganic halide perovskite quantum dots (QDs) have drawn attention as promising candidates for photodetectors, light-emitting diodes, and lasing applications. However, the sensitivity and instability of perovskite to moisture and heat seriously restrict their practical application to optoelectronic devices. Recently, a facile ligand-engineering strategy to suppress aggregation by replacing traditional long ligands oleylamine (OAm) during the hot injection process has been reported. Here, we further explore its thermal stability and the evolution of photoluminescence quantum yield (PLQY) under ambient environment. The modified $CsPbBr_3$ QDs film can maintain 33% of initial PL intensity, but only 17% is retained in the case of unmodified QDs after 10 h continuous heating. Further, the obtained QDs with higher initial PLQY (91.8%) can maintain PLQY to 39.9% after being continuously exposed in air for 100 days, while the PLQY of original QDs is reduced to 5.5%. Furthermore, after adhering $CsPbBr_3$ QDs on the surface of a micro SiO_2 sphere, we successfully achieve the highly-efficient upconversion random laser. In comparison with the unmodified $CsPbBr_3$ QDs, the laser from the modified $CsPbBr_3$ QDs presents a decreased threshold of 79.81 $\mu J/cm^2$ and higher quality factor (Q) of 1312. This work may not only provide a facile strategy to synthesize $CsPbBr_3$ QDs with excellent photochemical properties but also a bright prospect for high-performance random lasers.

https://doi.org/10.1364/PRJ.442659

1. INTRODUCTION

Owing to its outstanding optoelectronic properties, including flexible tunability of emission wavelength, long charge diffusion, high photoluminescence quantum yield (PLQY), large absorption coefficients, and narrow emission spectrum, all-inorganic halide perovskites nanomaterials $CsPbX_3$ (X = Br, Cl, or I) have drawn attention as promising candidates for next-generation photovoltaics [1–6], light emitters [7], photodetectors [8–11], etc., and particularly as an optical gain medium for lasers and amplified spontaneous emission (ASE) [12–17]. Historically, Kovalenko *et al.* first reported the ASE and lasing performance from $CsPbBr_3$ quantum dots (QDs) under femtosecond and nanosecond laser excitation [18]. Soon afterward, single-photon and two-photon pumped lasers of $CsPbBr_3$ QDs were demonstrated [19–21]. In addition, aiming at enhancing the lasing quality, reducing threshold, and improving the stability of $CsPbBr_3$, a series of studies have been conducted over the past few years [20–23].

Nevertheless, the sensitivity and instability of perovskite to moisture and heat seriously affect the performance of the perovskite lasers. To address these issues, diverse strategies such as coating, surface ligand engineering, and doping/alloying heterogeneous atoms have been implemented [24–28]. For example, our group devised an effective methodology to fabricate perovskite core/shell QDs by capping $CsPbBr_3$ QDs with CdS, resulting in ultrastability and nonblinking performance [29].

Mir *et al*. reported a doping method by using Mn and Yb to reduce defect density and improve stability [30]. However, the long-chain capping ligands including oleylamine (OAm) and oleic acid could still result in a nonradiative recombination of excitons and photoluminescence emission degradation, which largely affects the quality of perovskite lasers and further hinders their practical applications [31–35]. Therefore, among all these methods, the surface ligand modification in the synthesis process was vigorously promoted and developed. For instance, the surface of $CsPbBr_3$ QDs covered with ligands of different lengths can bring about different physical and chemical properties, including size, defect, stability, and so on [16,36,37]. However, among the previously reported methods, simple and effective strategies to improve not only photochemical properties of $CsPbBr_3$ QDs but also the performance of perovskite lasers remain scarce. Thus, it is necessary to explore a facile and low-cost method to fabricate $CsPbBr_3$ QDs for high-performance perovskite-based microlasers.

In view of previous studies, the weak binding energy between long-chain organic carbon chain ligands and QDs will lead to the aggregation of QDs and poor long-term stability, which has a great impact on the perovskite laser's performance [16,36–40]. A facile ligand-engineering strategy was proposed to promote properties of $CsPbBr_3$ QDs in our previous work by introducing the short-chain ligand octylamine (OLA) ligand ($CsPbBr_3$-OLA) to replace the traditional long ligands OAm ($CsPbBr_3$-OAm) during the hot injection process [22]. Based on this consequence, herein, we further explore its thermal stability and the evolution of photoluminescence quantum yield (PLQY) under ambient environment. The modified $CsPbBr_3$ QDs film can maintain 33% of initial PL intensity, but only 17% is retained in the case of unmodified QDs after

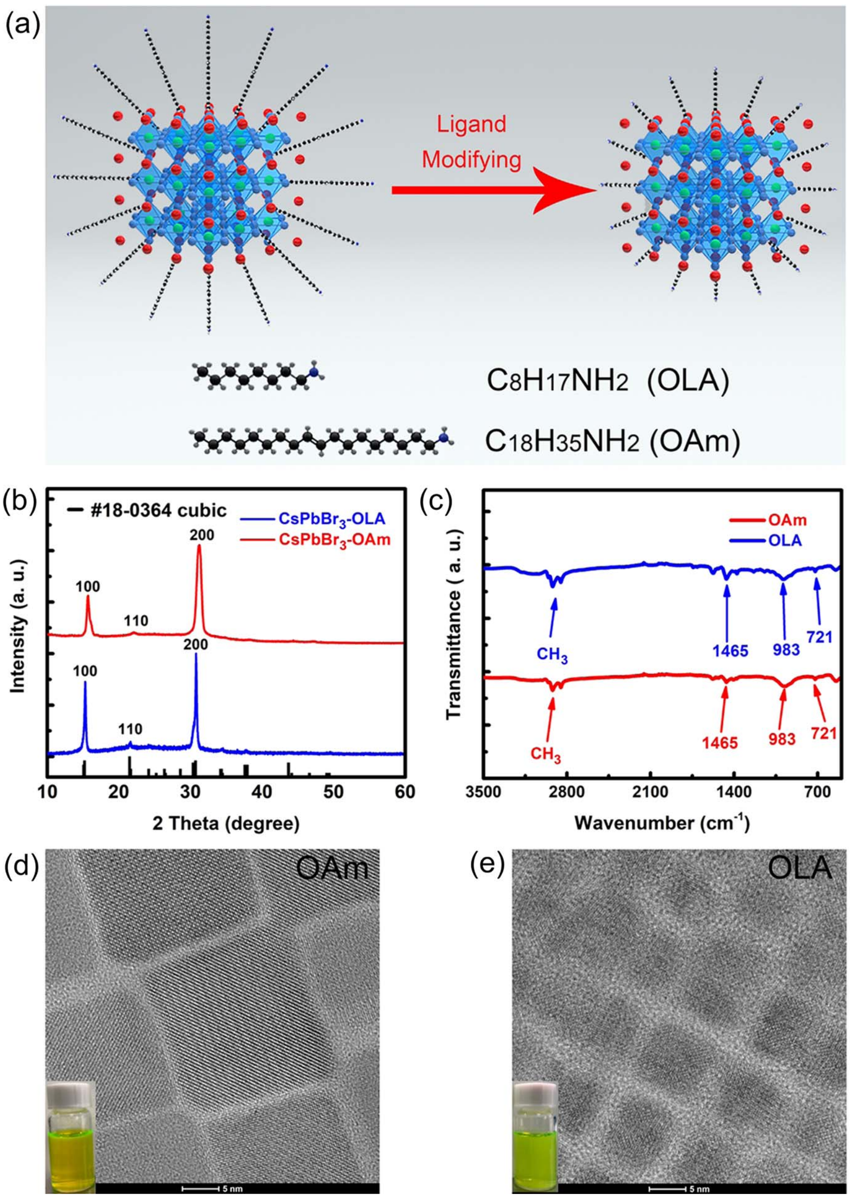

Fig. 1. (a) Passivation and ligand modification procedure on the surface of the $CsPbBr_3$ QDs. (b) XRD patterns and (c) FTIR spectra for $CsPbBr_3$ QDs with different ligands. HRTEM images for (d) $CsPbBr_3$-OAm and (e) $CsPbBr_3$-OLA QDs.

10 h continuous heating at 60°C. Further, the obtained QDs with higher initial PLQY (91.8%) can maintain PLQY to 39.9% after being continuously exposed in air for 100 days, while the PLQY of original QDs is reduced to 5.5%. Meanwhile, the synthesized $CsPbBr_3$-OLA QDs exhibit longer lifetime (16.90 ns) and no aggregation phenomenon after continuous exposure in air for 100 days. In addition, after coating $CsPbBr_3$ QDs onto the micro SiO_2 sphere, we finally succeeded in achieving the highly-efficient micro random lasers, and a lower threshold of 79.81 μJ/cm^2 and higher-quality factor (Q) of 1312 are presented from $CsPbBr_3$-OLA QDs. All these results indicate that a simple yet effective method to improve the properties of $CsPbBr_3$ QDs and the performance of perovskite microlasers has been realized. Simultaneously, it also provides a good prospect for the practical application of micro-nano semiconductor lasers.

2. EXPERIMENT

Cs_2CO_3 (cesium carbonate 81.5 mg, 0.25 mmol), ODE (octadecene 5 mL), and OA (oleic acid 0.5 mL) were mixed in a 100 mL three-neck flask. The mixture was heated to 120°C with magnetic stirring under flowing nitrogen and kept for 60 min until the solution became clear; then, the Cs precursor fluid was obtained. Meanwhile, $PbBr_2$ (lead bromide 138 mg) and ODE (10 mL) was added into a 100 mL three-neck flask, and the mixture were heated to 120°C with magnetic stirring and kept for 60 min, then OA (oleic acid, 1 mL) and OAm (oleylamine, 1 mL) were added in this solution; the temperature was then raised to 150°C and kept for 5 min until the solution became clear. The mixture (0.5 mL) was quickly injected into the Cs precursor fluid as soon as possible, and the temperature was maintained at 120°C for 5 s. The mixture was quickly cooled to room temperature by an ice-water bath after the reaction completed to produce OAm-$CsPbBr_3$ QDs. Finally, ethyl acetate was added into the crude solution with a volume ratio of 3:1; then, the mixed solution was put into a centrifuge with 6000 r/min for 5 min, and the precipitate was collected separately after centrifugation; finally, the sediment was dissolved into n-hexane. A similar procedure (replacing OAm with OLA, octylamine) was adopted for OLA-$CsPbBr_3$ QDs. All the above chemicals were purchased from Aladdin Chemistry Co., Ltd. (Shanghai, China).

$CsPbBr_3$ QDs were redispersed in n-hexane. 10 mg of commercial SiO_2 spheres was added in $CsPbBr_3$ QDs solution; the solution was then drop-coated onto the cleaned glass substrate for 60 min.

The QDs solution was dropped to the glass (15 mm × 15 mm) to study the properties of $CsPbBr_3$ QDs; the X-ray diffraction (XRD) pattern was collected by Cu Ka radiation (XRD-6100, Shimadzu, Japan). A Zeiss LIBRA 200FE microscope was used for TEM and high-resolution TEM images. The XPS profiles were tested by an ESCA Lab220I-XL. The FTIR spectra were obtained by an IRPrestige-21 spectrophotometer. The material absorption spectra were measured by a scan ultraviolet–visible spectrophotometer (ultraviolet-2100, ranging from 300 to 900 nm). The photoluminescence (PL) spectrum was obtained by a fluorescence spectrophotometer (Agilent Cary Eclipse, Australia). PL lifetime was obtained by a fluorescence spectrometer from Edinburgh Instruments (FS5-TCSPC). The PLQY was measured by an Edinburgh fluorescence spectrometer.

The fundamental pulse at 800 nm from a Ti:sapphire laser (repetition rate: 1 kHz, pulse-width: 35 fs, Solstice,

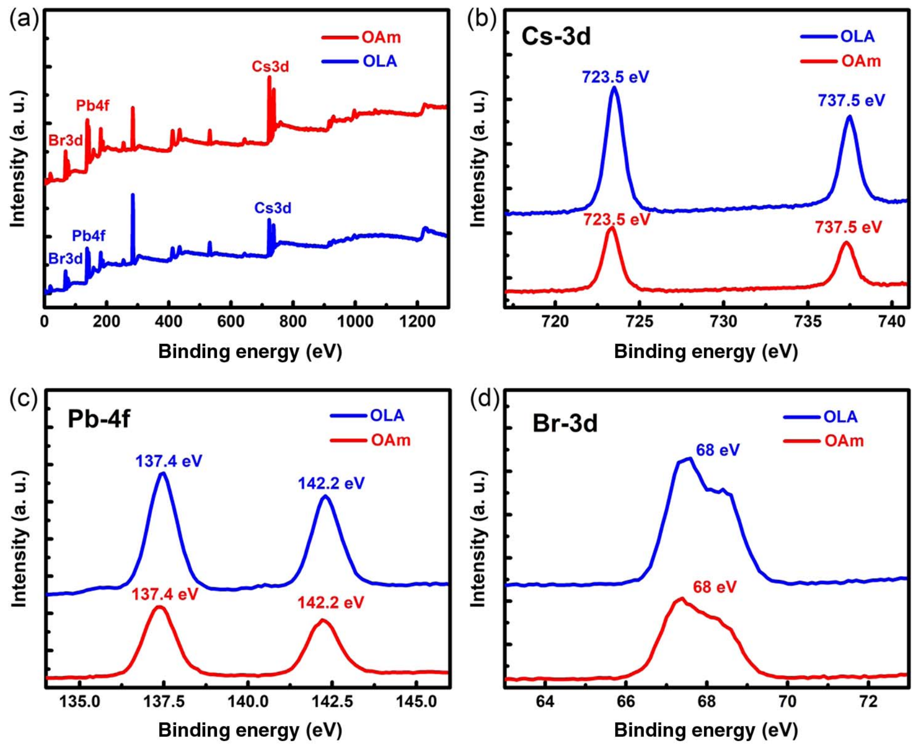

Fig. 2. (a) XPS profiles for $CsPbBr_3$-OAm and $CsPbBr_3$-OLA QDs, (b) Cs-3d spectrum, (c) Pb-4f spectrum, and (d) Br-3d spectrum.

Spectra-Physics) was used as a pump source. All the lasing experiments were carried out at room temperature.

3. RESULTS AND DISCUSSION

Traditional hot injection was adopted to synthesize $CsPbBr_3$ QDs, and lead bromide and cesium oleate were used as precursors [41]. In general, the long-chain ligand OAm is widely used during the synthesis process, which will result in intrinsic instability of $CsPbBr_3$ QDs [42–44]. Thus, OLA with the short carbon chain was used to replace the regular OAm ligand. The synthesis scheme of the engineered $CsPbBr_3$ QDs is schematically illustrated in Fig. 1(a). The X-ray diffraction (XRD) patterns of $CsPbBr_3$-OAm and $CsPbBr_3$-OLA QDs are shown in Fig. 1(b), confirming the cubic phase of $CsPbBr_3$ [45]. The main peaks are located at $2\theta = 15.2°$, 21.66°, and 30.69°, which correspond to the (100), (110), and (200) crystal planes of perovskite, respectively, indicating the excellent crystallization and pure phase of perovskite QDs. To investigate the surface ligand, the corresponding Fourier transform infrared (FTIR) spectra were measured, as shown in Fig. 1(c), and the peaks of CH_3 and CH_2 reveal that the $CsPbBr_3$ QDs are well capped with the OAm/OLA ligand after a purification process. There is no difference between $CsPbBr_3$-OAm and $CsPbBr_3$-OLA QDs, indicating that both have been successfully synthesized and well identified. In order to further study the morphological characteristics of perovskite QDs, transmission electron microscopy (TEM) was used to inspect the morphology and size distribution of QDs. High-resolution TEM (HRTEM) images for $CsPbBr_3$-OAm and $CsPbBr_3$-OLA QDs are displayed in Fig. 1(d) and Fig. 1(e), respectively. All QDs exhibit a cubic perovskite structure, high crystallinity, and good monodispersity. The average particle diameters of $CsPbBr_3$-OAm QDs and $CsPbBr_3$-OLA QDs are about 14

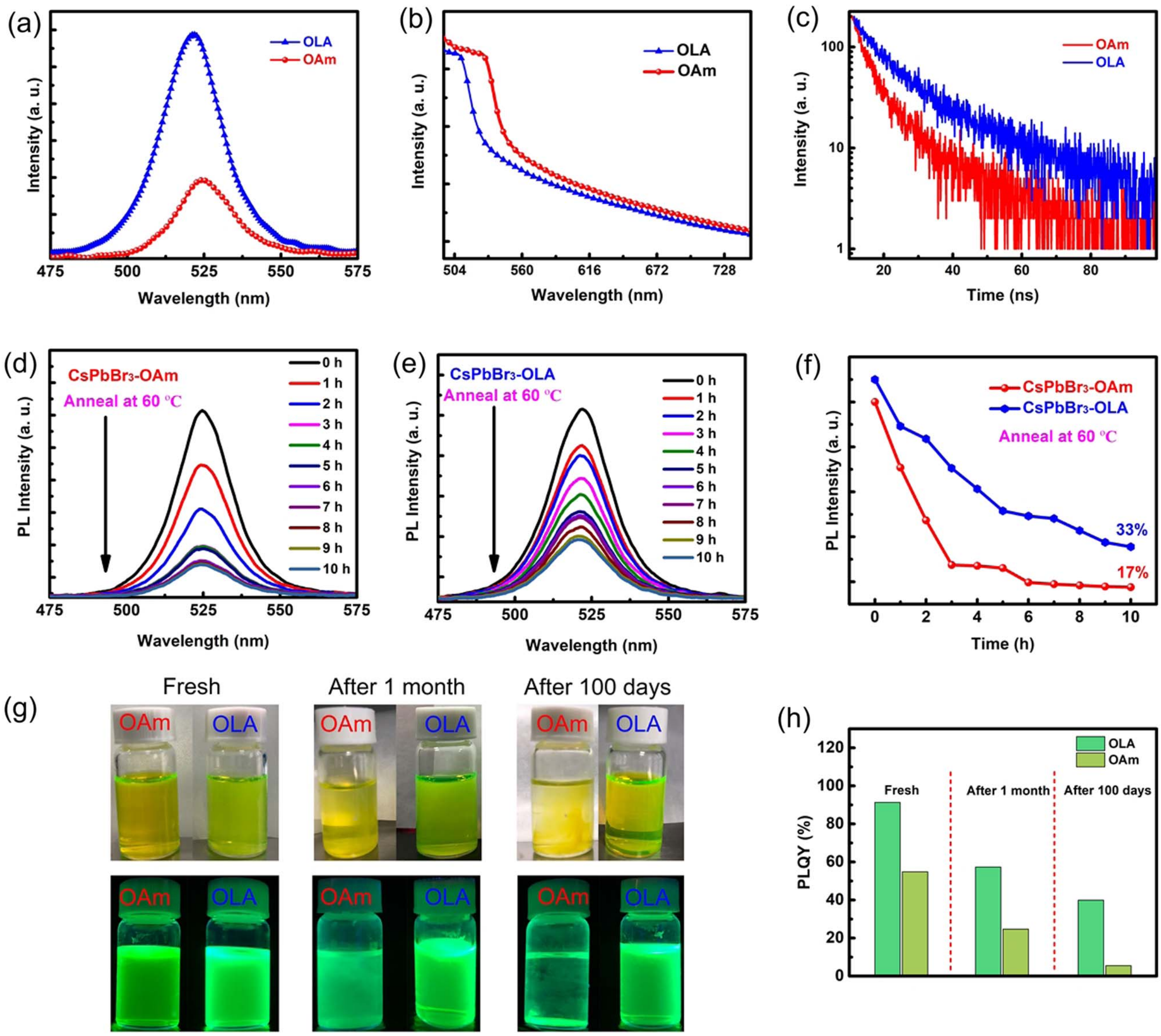

Fig. 3. (a) PL spectrum, (b) absorption spectrum, and (c) time-resolved PL decay of $CsPbBr_3$-OAm and $CsPbBr_3$-OLA QDs. PL stability measurement for (d) $CsPbBr_3$-OAm and (e) $CsPbBr_3$-OLA QDs under heating conditions. (f) PL intensity variation of QDs films over 10 h under heating conditions. (g) Photographs under daylight and 365 nm UV light of $CsPbBr_3$-OAm and $CsPbBr_3$-OLA QDs for 100 days in hexane. (h) PLQY variation of QDs solution in air over 100 days.

Table 1. Time-Resolved PL Decays for $CsPbBr_3$-OLA QDs and $CsPbBr_3$-OAm QDs

	τ_1 (ns)	A_1 (%)	τ_2 (ns)	A_2 (%)	τ_a (ns)
OLA-QDs	3.4	157.9	14.6	44.8	9.5
OAm-QDs	5.8	113.7	21.2	80.1	16.9

and 8 nm, respectively. The smaller size of $CsPbBr_3$-OLA QDs could be ascribed to the short allylic ligands, which would result in weaker attractive van der Waals (VDW) interactions with each other than the long ones [46]. Meanwhile, Fig. 2(a) displays an X-ray photoelectron spectroscopy (XPS) profile of perovskite QDs, and the Cs 3d peaks at 724 and 738 eV, Pb 4f peaks at 138 and 143 eV, and Br 3d peaks at 68 eV can be observed in the Figs. 2(b)–2(d). All the above experimental results confirm the successful synthesis of the $CsPbBr_3$ QDs.

To explore the effect of ligand modification on the emitting properties of the $CsPbBr_3$ QDs, we investigated the absorption, photoluminescence (PL) spectra, and lifetime of $CsPbBr_3$-OAm and $CsPbBr_3$-OLA QDs films. Figure 3(a) shows the center of PL spectrum peak of $CsPbBr_3$-OAm and $CsPbBr_3$-OLA QDs is around 524 and 520 nm, respectively. Because of quantum confinement effect, the PL spectrum of $CsPbBr_3$-OLA is blueshifted [22,23]. The corresponding absorption peaks of the sample in Fig. 3(b) appear at about 517 and 511 nm, presenting a slight Stokes shift [47]. Time-resolved PL decays were conducted to understand the carrier dynamics, and the PL decay curves of both QDs are displayed in Fig. 3(c). After fitted with a bi-exponential decay function, fast-decay component (τ_1), slow-decay component (τ_2), and calculated average lifetimes (τ_a) are as summarized in Table 1. The average PL lifetimes of $CsPbBr_3$-OLA and $CsPbBr_3$-OAm QDs are 16.7 and 9.54 ns, respectively. The prolonged lifetime of $CsPbBr_3$-OLA QDs implies that OLA can effectively decrease the surface defects of QDs and benefit nonradiative recombination suppression assisted by the defect [48].

As shown in Fig. 3(d), the PL intensity of $CsPbBr_3$-OAm QDs film decreases quickly for 10 h under the annealing at 60°C, while the PL intensity of $CsPbBr_3$-OLA QDs film displays a slow decrease under the same condition in Fig. 3(e). The overall tendency is summarized in the Fig. 3(f). Although PL intensity of both types of the QDs films exhibits a downward trend over time, the $CsPbBr_3$-OLA QDs film can maintain 33% of initial PL intensity, but only 17% is retained in the case of $CsPbBr_3$-OLA QDs after 10 h continuous heating, illustrating that the $CsPbBr_3$-OLA QDs film possesses better heat tolerance. Figure 3(g) shows the photographs of $CsPbBr_3$-OAm and $CsPbBr_3$-OLA QDs in a hexane solution for 100 days under daylight and an ultraviolet (UV) lamp. The initial solutions of two types QDs are clear and highly bright. After stored in ambient for 100 days, the $CsPbBr_3$-OAm QDs solution has aggregated and degraded, while the solution of $CsPbBr_3$-OLA QDs still exhibits high luminescent brightness after 100 days. Meanwhile, we investigated the change of PLQY during 100 days; as shown in Fig. 3(h), the initial PLQY of $CsPbBr_3$-OLA QDs is as high as 91.3%. The PLQY of $CsPbBr_3$-OAm QDs has decreased to only 5.5% after being continuously exposed in air for more than 100 days, while the PLQY still remains 39.9% for $CsPbBr_3$-OLA QDs, indicating better chemical stability in air, and it is beneficial to practical applications in future.

Previously, all-inorganic $CsPbX_3$ perovskites have been reported as having excellent potential as candidates for nanolasers

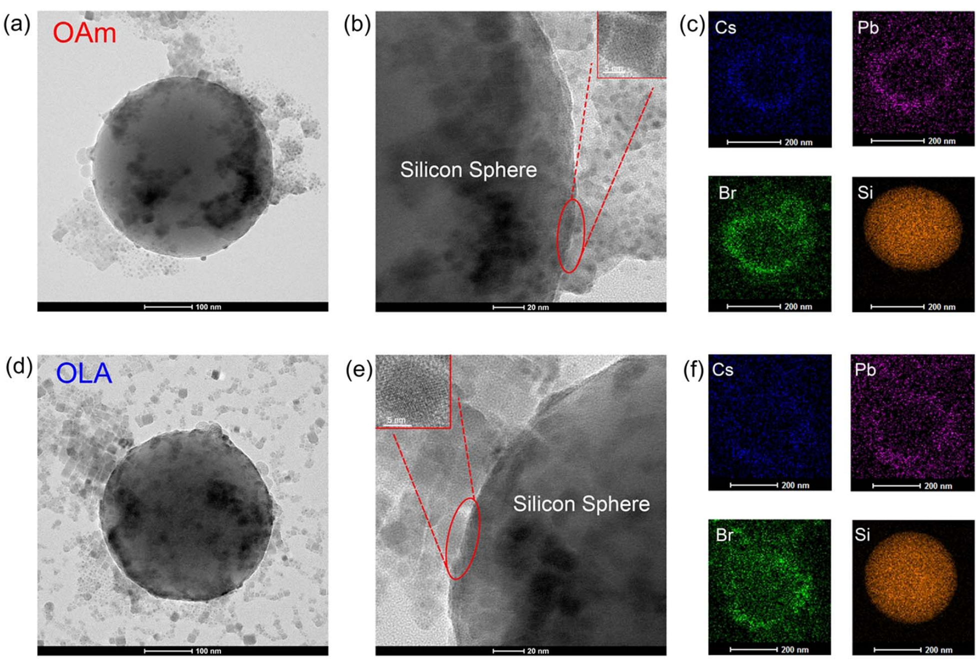

Fig. 4. (a) TEM image, (b) HRTEM image, and (c) element mapping of $CsPbBr_3$-OAm/SiO_2 composite. (d) TEM image, (e) HRTEM image, and (f) element mapping of $CsPbBr_3$-OLA/SiO_2 composite.

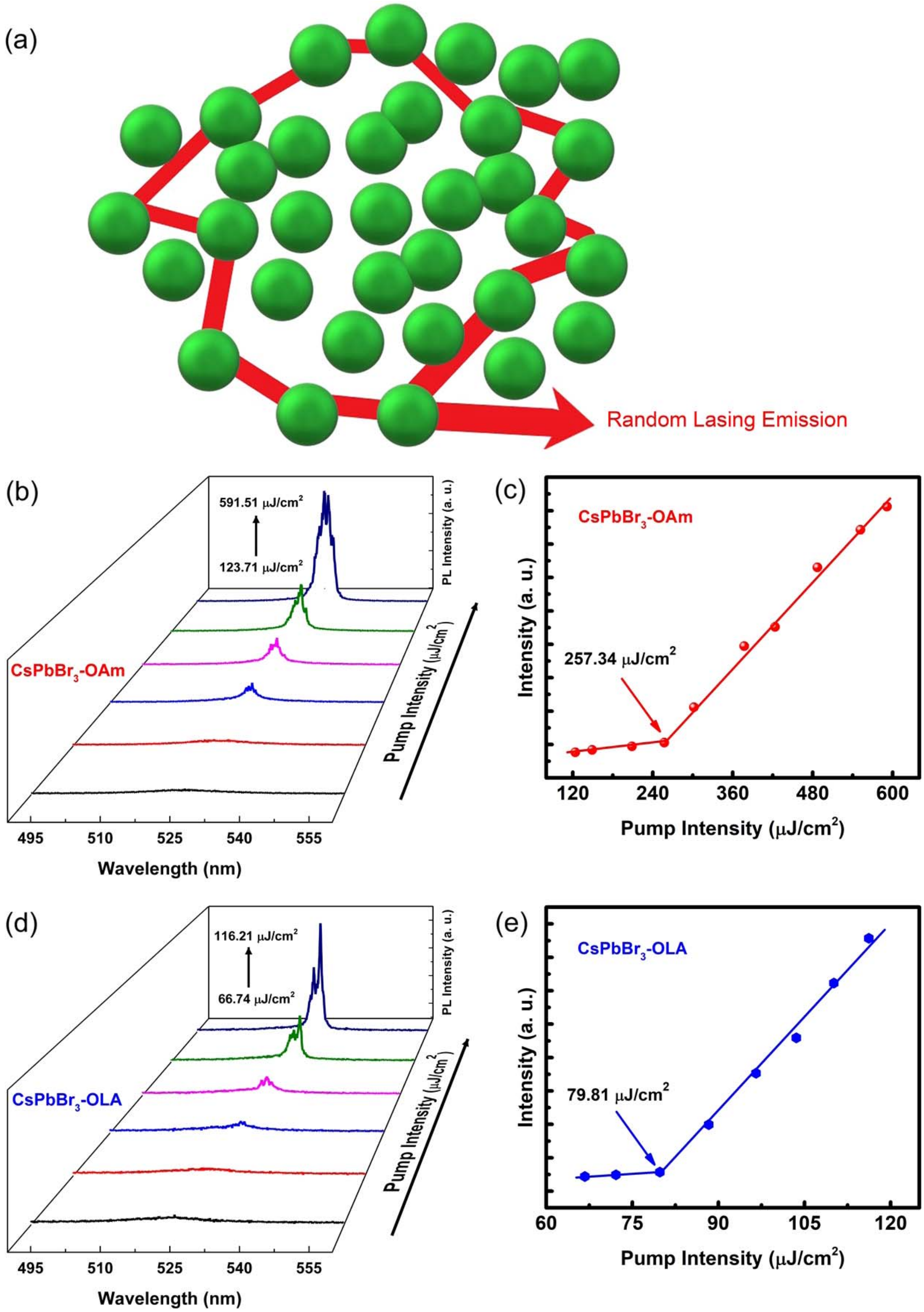

Fig. 5. Random lasing from the composite film under two-photon excitation. (a) Schematic of random lasing from $CsPbBr_3/SiO_2$ composite film upon 800 nm excitation above lasing threshold. (b) Power-dependent emission spectra from $CsPbBr_3$-OAm/SiO_2 composite film. (c) Integrated lasing intensity of $CsPbBr_3$-OAm/SiO_2 composite film as a function of power fluence showing the lasing threshold at 257.34 $\mu J/cm^2$. (d) Power-dependent emission spectra from $CsPbBr_3$-OLA/SiO_2 composite film. (e) Integrated lasing intensity of $CsPbBr_3$-OLA/SiO_2 composite film as a function of power fluence showing the lasing threshold at 79.81 $\mu J/cm^2$.

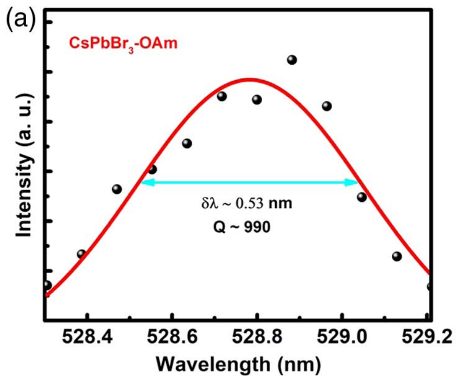

Fig. 6. Gaussian fitting of a selected lasing peak corresponding to the Q-value from (a) $CsPbBr_3$-OAm/SiO_2 and (b) $CsPbBr_3$-OLA/SiO_2.

[39,45]. To explore the lasing performance before and after modification, a commercial silica sphere (SiO_2) was adopted. $CsPbBr_3$-OAm QDs and $CsPbBr_3$-OLA QD were coated on the surface of the SiO_2 to form composites ($CsPbBr_3$-OAm/SiO_2 and $CsPbBr_3$-OLA/SiO_2), respectively. Specific experimental methods can be seen in the experimental section. Figure 4(a) presents the TEM image of a micro SiO_2 sphere covered with $CsPbBr_3$-OAm QDs; the average diameter of the SiO_2 sphere can be observed to be about 200 nm. The HRTEM image is displayed in Fig. 4(b); the lattice fringe of the QDs can be clearly observed, indicating the existence of QDs on the surface of the SiO_2 sphere. To further study the chemical composition of $CsPbBr_3$-OAm/SiO_2, energy-dispersive spectrometer (EDS) mapping was performed, as shown in Fig. 4(c), which illustrates uniform and effective distribution of the Cs, Pb, Br, and Si atoms coated on SiO_2 sphere. Moreover, the corresponding TEM, HRTEM, and EDS mapping analyses based on the $CsPbBr_3$-OLA/SiO_2 composite are shown in Figs. 4(d)–4(f), respectively. All the above experimental results demonstrate that a composite structure between the perovskite QDs and silica beads is successfully formed, providing a good foundation for further laser output.

To study the lasing properties, the well-dispersed $CsPbBr_3$/SiO_2 composite was transferred from the solution to the glass substrates. Subsequently, the close-packed thin film of $CsPbBr_3$/SiO_2 composite was pumped by an 800 nm femtosecond laser with 35 fs pulses at a repetition rate of 1 kHz under ambient conditions. The schematic of random lasing from $CsPbBr_3$/SiO_2 composite film is depicted in Fig. 5(a). The typical excitation fluence-dependent PL spectra of the $CsPbBr_3$-OAm/SiO_2 composite are displayed in Fig. 5(b), and the lasing behavior has been achieved at various pump excitation. Below the lasing threshold, only a broad spontaneous emission centered at ~525 nm with a full-width at half-maximum (FWHM) of ~25 nm can be observed. Strikingly, as the pumping intensity increases to exceed a threshold of 257.34 μJ/cm^2, multiple sharp peaks emerge at the low-energy shoulders of the spontaneous emission spectrum and the FWHM decreases dramatically, elucidating that the lasing action was occurring. Additionally, the laser peak position is irregularly changed, and the spacing between adjacent peaks is also not fixed, which is evidence of random laser generation [44]. Figure 5(c) shows the slopes of the output intensity versus pump fluence from $CsPbBr_3$-OAm/SiO_2 composite, and the lasing threshold value is determined to be 257.34 μJ/cm^2, which also reveals the transition from spontaneous emission to stimulated emission as the pump intensity increases [13,18]. Similarly, the laser behavior with analogous characteristic from the $CsPbBr_3$-OLA QDs layer onto SiO_2 can be observed in Fig. 5(d). Furthermore, as shown in Fig. 5(e), the lasing threshold of $CsPbBr_3$-OLA/SiO_2 composite is only 79.81 μJ/cm^2, which is less than one-third of the $CsPbBr_3$-OAm/SiO_2 composite. To further analyze the performance of a random laser, Q-factor analysis of $CsPbBr_3$/SiO_2 composite film was conducted. The relationship $Q = \frac{\lambda}{\delta\lambda}$ is used to estimate the Q-factor in our experiment, where λ is the center wavelength of lasing and $\delta\lambda$ is the FWHM value. The calculated results can be seen in Fig. 6; the Q-factor of $CsPbBr_3$-OAm/SiO_2 is only 990, while the Q-factor of $CsPbBr_3$-OAm/SiO_2 is as high as 1312. All these aforementioned consequences illustrate a promising development of low-threshold random upconverted laser with all-inorganic perovskite QDs.

4. CONCLUSION

In summary, a facile and valid ligand modification strategy is proposed to synthesize $CsPbBr_3$ QDs with better photochemical properties. The obtained perovskite QDs exhibit longer lifetime, higher PLQY, and better stability to moisture and heat. In addition, we coat $CsPbBr_3$ QDs on the surface of the SiO_2 to form composites and realize a random laser from $CsPbBr_3$/SiO_2 composite under ambient conditions. In comparison with $CsPbBr_3$-OAm/SiO_2 composites, the laser of $CsPbBr_3$-OLA/SiO_2 composites presents lower threshold (79.81 μJ/cm^2) and higher Q-factor (1312) under two-photon (800 nm) excitation. This work would provide a novel and feasible strategy for the remarkable upconversion random lasers and promote the development of microlasers with all-inorganic perovskite QDs.

Funding. China Postdoctoral Science Foundation (2020M681421); CAS Interdisciplinary Innovation Team, International ST Cooperation Program of China (2016YFE0119300); Program of Shanghai Academic

Research Leader (18XD1404200); National Natural Science Foundation of China (61875211, 61905264, 61925507, 62005296, 92050203); National Key R&D Program of China (2017YFE0123700).

Disclosures. The authors declare no conflicts of interest.

REFERENCES

1. X. Li, Y. Wu, S. Zhang, B. Cai, Y. Gu, J. Song, and H. Zeng, "$CsPbX_3$ quantum dots for lighting and displays: room-temperature synthesis, photoluminescence superiorities, underlying origins and white light emitting diodes," Adv. Funct. Mater. **26**, 2435–2445 (2016).
2. L. Protesescu, S. Yakunin, M. I. Bodnarchuk, F. Krieg, R. Caputo, C. H. Hendon, R. X. Yang, A. Walsh, and M. V. Kovalenko, "Nanocrystals of cesium lead halide perovskites ($CsPbX_3$, X = Cl, Br, and I): novel optoelectronic materials showing bright emission with wide color gamut," Nano Lett. **15**, 3692–3696 (2015).
3. J. Song, J. Li, X. Li, L. Xu, Y. Dong, and H. Zeng, "Nanocrystals: quantum dot light-emitting diodes based on inorganic perovskite cesium lead halides ($CsPbX_3$)," Adv. Mater. **27**, 7162–7167 (2015).
4. X. Du, G. Wu, J. Cheng, H. Dang, K. Ma, Y.-W. Zhang, P.-F. Tan, and S. Chen, "High quality $CsPbBr_3$ perovskite nanocrystals for quantum dot light-emitting diodes," RSC Adv. **7**, 10391–10396 (2017).
5. J. Li, L. Xu, T. Wang, J. Song, J. Chen, J. Xue, Y. Dong, B. Cai, Q. Shan, B. Han, and H. Zeng, "50-fold EQE improvement up to 6.27% of solution-processed all-inorganic perovskite $CsPbBr_3$ QLEDs via surface ligand density control," Adv. Mater. **29**, 1603885 (2017).
6. A. Swarnkar, A. R. Marshall, E. M. Sanehira, B. D. Chernomordik, D. T. Moore, J. A. Christians, T. Chakrabarti, and J. M. Luther, "Quantum dot–induced phase stabilization of α-$CsPbI_3$ perovskite for high-efficiency photovoltaics," Science **354**, 92–95 (2016).
7. M. Yuan, L. N. Quan, R. Comin, G. Walters, R. Sabatini, O. Voznyy, S. Hoogland, Y. Zhao, E. M. Beauregard, P. Kanjanaboos, Z. Lu, D. H. Kim, and E. H. Sargent, "Perovskite energy funnels for efficient light-emitting diodes," Nat. Nanotechnol. **11**, 872–877 (2016).
8. Q. Chen, J. Wu, X. Ou, B. Huang, J. Almutlaq, A. A. Zhumekenov, X. Guan, S. Han, L. Liang, Z. Yi, J. Li, X. Xie, Y. Wang, Y. Li, D. Fan, D. B. L. Teh, A. H. All, O. F. Mohammed, O. M. Bakr, T. Wu, M. Bettinelli, H. Yang, W. Huang, and X. Liu, "All-inorganic perovskite nanocrystal scintillators," Nature **561**, 88–93 (2018).
9. Y. Chen, Y. Chu, X. Wu, W. Ou-Yang, and J. Huang, "High-performance inorganic perovskite quantum dot-organic semiconductor hybrid phototransistors," Adv. Mater. **29**, 1704062 (2017).
10. X. Song, X. Liu, D. Yu, C. Huo, J. Ji, X. Li, S. Zhang, Y. Zou, G. Zhu, Y. Wang, M. Wu, A. Xie, and H. Zeng, "Boosting two-dimensional MoS_2/$CsPbBr_3$ photodetectors via enhanced light absorbance and interfacial carrier separation," ACS Appl. Mater. Interfaces **10**, 2801–2809 (2018).
11. Y. Dong, Y. Zou, J. Song, X. Song, and H. Zeng, "Recent progress of metal halide perovskite photodetectors," J. Mater. Chem. C **5**, 11369–11394 (2017).
12. Z. Yong, Y. Zhou, J. Ma, Y. Chen, J. Yang, Y. Song, J. Wang, and H. Sun, "Controlling crystallization of all-inorganic perovskite films for ultralow-threshold amplification spontaneous emission," ACS Appl. Mater. Interfaces **9**, 32920–32929 (2017).
13. Y. Wang, X. Li, X. Zhao, L. Xiao, H. Zeng, and H. Sun, "Nonlinear absorption and low-threshold multiphoton pumped stimulated emission from all-inorganic perovskite nanocrystals," Nano Lett. **16**, 448–453 (2016).
14. Z. Hu, Z. Liu, Z. Zhan, T. Shi, J. Du, X. Tang, and Y. Leng, "Advances in metal halide perovskite lasers: synthetic strategies, morphology control, and lasing emission," Adv. Photon. **3**, 034002 (2021).
15. Y. Xu, Q. Chen, C. Zhang, R. Wang, H. Wu, X. Zhang, G. Xing, W. W. Yu, X. Wang, Y. Zhang, and M. Xiao, "Two-photon-pumped perovskite semiconductor nanocrystal lasers," J. Am. Chem. Soc. **138**, 3761–3768 (2016).
16. S. W. Eaton, M. Lai, N. A. Gibson, A. B. Wong, L. Dou, J. Ma, L.-W. Wang, S. R. Leone, and P. Yang, "Lasing in robust cesium lead halide perovskite nanowires," Proc. Natl. Acad. Sci. USA **113**, 1993–1998 (2016).
17. Z. Liu, M. Hu, J. Du, T. Shi, Z. Wang, Z. Zhang, Z. Hu, Z. Zhan, K. Chen, W. Liu, J. Tang, H. Zhang, Y. Leng, and R. Li, "Subwavelength-polarized quasi-two-dimensional perovskite single-mode nanolaser," ACS Nano **15**, 6900–6908 (2021).
18. S. Yakunin, L. Protesescu, F. Krieg, M. I. Bodnarchuk, G. Nedelcu, M. Humer, G. De Luca, M. Fiebig, W. Heiss, and M. V. Kovalenko, "Low threshold amplified spontaneous emission and lasing from colloidal nanocrystals of cesium lead halide perovskites," Nat. Commun. **6**, 8056 (2015).
19. J. Pan, S. P. Sarmah, B. Murali, I. Dursun, W. Peng, M. R. Parida, J. Liu, L. Sinatra, N. Alyami, C. Zhao, E. Alarousu, T. K. Ng, B. S. Ooi, O. M. Bakr, and O. F. Mohammed, "Air-stable surface-passivated perovskite quantum dots for ultra-robust, single- and two-photon-induced amplified spontaneous emission," J. Phys. Chem. Lett. **6**, 5027–5033 (2015).
20. X. Chen, K. Wang, B. Shi, T. Liu, R. Chen, M. Zhang, W. Wen, G. Xing, and J. Wu, "All-inorganic perovskite nanorod arrays with spatially randomly distributed lasing modes for all-photonic cryptographic primitives," ACS Appl. Mater. Interfaces **13**, 30891–30901 (2021).
21. Y. Lu, T. L. Shen, K. Peng, P. Cheng, S. Chang, M. Lu, C. W. Chu, T. Guo, and H. A. Atwater, "Up conversion plasmonic lasing from an organolead trihalide perovskite nanocrystal with low threshold," ACS Photon. **8**, 335–342 (2021).
22. Q. Xiong, S. Huang, J. Du, X. Tang, F. Zeng, Z. Liu, Z. Zhang, T. Shi, J. Yang, D. Wu, H. Lin, Z. Luo, and Y. Leng, "Surface ligand engineering for $CsPbBr_3$ quantum dots aiming at aggregation suppression and amplified spontaneous emission improvement," Adv. Opt. Mater. **8**, 2000977 (2020).
23. Y. Wang, M. Zhi, Y. Chang, J. Zhang, and Y. Chan, "Stable, ultralow threshold amplified spontaneous emission from $CsPbBr_3$ nanoparticles exhibiting trion gain," Nano Lett. **18**, 4976–4984 (2018).
24. Z.-J. Li, E. Hofman, J. Li, A. H. Davis, C.-H. Tung, L.-Z. Wu, and W. Zheng, "Photoelectrochemically active and environmentally stable $CsPbBr_3$/TiO_2 core/shell nanocrystals," Adv. Funct. Mater. **28**, 1704288 (2018).
25. S. Wang, J. Yu, M. Zhang, D. Chen, C. Li, R. Chen, G. Jia, A. L. Rogach, and X. Yang, "Stable, strongly emitting cesium lead bromide perovskite nanorods with high optical gain enabled by an intermediate monomer reservoir synthetic strategy," Nano Lett. **19**, 6315–6322 (2019).
26. H. C. Wang, S. Y. Lin, A. C. Tang, B. P. Singh, H. C. Tong, C. Y. Chen, Y. C. Lee, T. L. Tsai, and R. S. Liu, "Mesoporous silica particles integrated with all-inorganic $CsPbBr_3$ perovskite quantum-dot nanocomposites (MP-PQDs) with high stability and wide color gamut used for backlight display," Angew. Chem. **55**, 7924–7929 (2016).
27. X. Liu, X. Zhang, L. Li, J. Xu, S. Yu, X. Gong, J. Zhang, and H. Yin, "Stable luminescence of $CsPbBr_3$/nCdS core/shell perovskite quantum dots with Al self-passivation layer modification," ACS Appl. Mater. Interfaces **11**, 40923–40931 (2019).
28. T. Xuan, X. Yang, S. Lou, J. Huang, Y. Liu, J. Yu, H. Li, K. L. Wong, C. Wang, and J. Wang, "Highly stable $CsPbBr_3$ quantum dots coated with alkyl phosphate for white light-emitting diodes," Nanoscale **9**, 15286–15290 (2017).
29. X. Tang, J. Yang, S. Li, Z. Liu, Z. Hu, J. Hao, J. Du, Y. Leng, H. Qin, X. Lin, Y. Lin, Y. Tian, M. Zhou, and Q. Xiong, "Single halide perovskite/semiconductor core/shell quantum dots with ultrastability and non-blinking properties," Adv. Sci. **6**, 1900412 (2019).
30. W. J. Mir, Y. Mahor, A. Lohar, M. Jagadeeswararao, S. Das, S. Mahamuni, and A. Nag, "Postsynthesis doping of Mn and Yb into $CsPbX_3$ (X = Cl, Br, or I) perovskite nanocrystals for down-conversion emission," Chem. Mater. **30**, 8170–8178 (2018).
31. F. Krieg, S. T. Ochsenbein, S. Yakunin, S. ten Brinck, P. Aellen, A. Sness, B. Clerc, D. Guggisberg, O. Nazarenko, Y. Shynkarenko, S. Kumar, C. J. Shih, I. Infante, and M. V. Kovalenko, "Colloidal $CsPbX_3$ (X = Cl, Br, I) nanocrystals 2.0: Zwitterionic capping ligands for improved durability and stability," ACS Energy Lett. **3**, 641–646 (2018).
32. V. K. Ravi, P. K. Santra, N. Joshi, J. Chugh, S. K. Singh, H. Rensmo, P. Ghosh, and A. Nag, "Origin of the substitution mechanism for the

binding of organic ligand on the surface of $CsPbBr_3$ perovskite nanocubes," J. Phys. Chem. Lett. **8**, 4988–4994 (2017).
33. C. Dong, Y. Xiao, Z. Han, G. Guo, X. Jiang, L. Tong, C. Gu, and H. Ming, "Low-threshold microlaser in Er:Yb phosphate glass coated microsphere," IEEE Photon. Technol. Lett. **20**, 342–344 (2008).
34. X. Li, F. Cao, D. Yu, J. Chen, Z. Sun, Y. Shen, Y. Zhu, L. Wang, Y. Wei, Y. Wu, and H. Zeng, "All inorganic halide perovskites nanosystem: synthesis, structural features, optical properties and optoelectronic applications," Small **13**, 1603996 (2017).
35. A. Pan, B. He, X. Fan, Z. Liu, J. J. Urban, A. P. Alivisatos, L. He, and Y. Liu, "Insight into the ligand-mediated synthesis of colloidal $CsPbBr_3$ perovskite nanocrystals: the role of organic acid, base, and cesium precursors," ACS Nano **10**, 7943–7954 (2016).
36. M. L. De Giorgi, F. Krieg, M. V. Kovalenko, and M. Anni, "Amplified spontaneous emission threshold reduction and operational stability improvement in $CsPbBr_3$ nanocrystals films by hydrophobic functionalization of the substrate," Sci. Rep. **9**, 17964 (2019).
37. K. Ren, J. Wang, S. Chen, Q. Yang, J. Tian, H. Yu, M. Sun, X. Zhu, S. Yue, Y. Sun, K. Liu, M. Azam, Z. Wang, P. Jin, S. Qu, and Z. Wang, "Realization of perovskite-nanowire-based plasmonic lasers capable of mode modulation," Laser Photon. Rev. **13**, 1800306 (2019).
38. Y.-F. Xiao, B.-B. Li, X. Jiang, X. Hu, Y. Li, and Q. Gong, "High quality factor, small mode volume, ring-type plasmonic micro resonator on a silver chip," J. Phys. B **43**, 035402 (2010).
39. H. Zhu, Y. Fu, F. Meng, X. Wu, Z. Gong, Q. Ding, M. V. Gustafsson, M. T. Trinh, S. Jin, and X. Y. Zhu, "Lead halide perovskite nanowire lasers with low lasing thresholds and high quality factors," Nat. Mater. **14**, 636–642 (2015).
40. D. Yan, T. Shi, Z. Zang, T. Zhou, Z. Liu, Z. Zhang, J. Du, Y. Leng, and X. Tang, "Ultrastable $CsPbBr_3$ perovskite quantum dot and their enhanced amplified spontaneous emission by surface ligand modification," Small **15**, 1901173 (2019).
41. W. Yang, L. Fei, F. Gao, W. Liu, H. Xu, L. Yang, and Y. Liu, "Thermal polymerization synthesis of $CsPbBr_3$ perovskite-quantum-dots@copolymer composite: towards long-term stability and optical phosphor application," Chem. Eng. J. **387**, 124180 (2020).
42. A. Mikosch, S. Ciftci, G. Tainter, R. Shivanna, B. Haehnle, F. Deschler, and A. J. C. Kuehne, "Laser emission from self-assembled colloidal crystals of conjugated polymer particles in a metal-halide perovskite matrix," Chem. Mater. **31**, 2590–2596 (2019).
43. H. Zhang, L. Yuan, Y. Chen, Y. Zhang, Y. Yu, X. Liang, W. Xiang, and T. Wang, "Amplified spontaneous emission and random lasing using $CsPbBr_3$ quantum dot glass through controlling crystallization," Chem. Commun. **56**, 2853–2856 (2020).
44. S. Yuan, D. Chen, X. Li, J. Zhong, and X. Xu, "*In situ* crystallization synthesis of $CsPbBr_3$ perovskite quantum dot-embedded glasses with improved stability for solid-state lighting and random upconverted lasing," ACS Appl. Mater. Interfaces **10**, 18918–18926 (2018).
45. S. Liu, G. Shao, L. Ding, J. Liu, W. Xiang, and X. Liang, "Sn-doped $CsPbBr_3$ QDs glass with excellent stability and optical properties for WLED," Chem. Eng. J. **361**, 937–944 (2019).
46. S. Aharon, M. Wierzbowska, and L. Etgar, "The effect of the alkylammonium ligand's length on organic–inorganic perovskite nanoparticles," ACS Energy Lett. **3**, 1387–1393 (2018).
47. M. C. Brennan, J. E. Herr, T. S. Nguyen-Beck, J. Zinna, S. Draguta, S. Rouvimov, J. Parkhill, and M. Kuno, "Origin of the size-dependent Stokes shift in $CsPbBr_3$ perovskite nanocrystals," J. Am. Chem. Soc. **139**, 12201–12208 (2017).
48. A. Chiasera, Y. Dumeige, P. Féron, M. Ferrari, Y. Jestin, G. N. Conti, S. Pelli, S. Soria, and G. C. Righini, "Spherical whispering-gallery-mode microresonators," Laser Photon. Rev. **4**, 457–482 (2010).